Improving the Dimming Performance of Low-Power Single-Stage AC–DC HBLED Drivers

Mirko Bodetto, Abdelali El Aroudi, *Senior Member, IEEE*, Angel Cid-Pastor, *Member, IEEE*, and Mohammed S. Al-Numay, *Member, IEEE*

***Abstract*—The design of efficient single-stage high-brightness light-emitting diodes (HBLEDs) ac–dc drivers with power factor correction (PFC) in low-power applications is addressed in this paper. The PFC is achieved by using a switching converter with both step-up and step-down voltage capability. It is well known that a good tracking of the input reference current close to the zero crossing is challenging, in particular when the LED output current is low, hence jeopardizing the power quality at low power levels. A solution is proposed to improve the power quality in ac–dc LED drivers under inner current loop based on a variable hysteresis modulation scheme. An adaptive hysteresis window modulated by the input voltage and the output LED current reference is used. The double modulation strategy helps to avoid the distortion near the zero crossings of the input current and to improve the dimming performance of the HBLEDs. This results in a low value of total harmonic distortion (THD) under low current/power conditions and therefore in a very good dimming performance in single-stage ac–dc HBLEDs drivers with PFC. The operation principle of the proposed technique is presented and numerical simulations are shown to demonstrate its functionality. A laboratory prototype is designed and tested to verify its feasibility obtaining a significant improvement in terms of power quality. Under universal input voltage operation, good efficiency and low THD can be achieved even for low power levels.**

***Index Terms*—AC–DC power converters, dimming, LED lamps, lighting control, power factor correction (PFC).**

I. Introduction

SOLID-STATE light is of significant interest in modern lighting applications. In particular high-brightness light-emitting diodes (HBLEDs) provide comparable efficacy to high-efficiency discharge lamps with the added advantages of no use of mercury, long lifetime, low-operating voltages, and compact size [1]–[3]. All of this gives an additional incentive to use these devices, and they are quickly replacing halogen and compact fluorescents lamps in residential, commercial, and industrial applications [4]–[8]. In addition a significant improvement in thermal design [9]–[11] and a decrease in manufacturing cost are already obtained in HBLED technology making them competitive with many other kinds of lamps. Therefore, they are considered as the future trend in lighting applications such as in modern vehicles lights, homes, street lighting, traffic, and commercial signs among others.

Nevertheless, it has to be taken into account that LED drivers cannot be as simple as those of the incandescent lamps. A drawback is presented in the relationship between temperature, luminous flux, and current. In [12]–[16] details of the problems caused by the temperature and the consequent effect on performance and lifetime of the LEDs are presented. In addition, the requirements regarding voltage and current are completely different from the rest of lighting devices. HBLEDs are based on semiconductors thus requiring a dc supply current. Considering the high efficiency obtained in these HBLEDs, its adaptation stage must have a similar performance in terms of conversion efficiency. High efficiency, high power density, and high control accuracy can be achieved with switching power supplies. Power quality is also a key issue in LED drivers. High total harmonic distortion (THD) due to low power quality can provoke an annoying lamp flickering apart from causing serious problems on the ac line. Hence, for LED drivers that use an ac input source, an ac–dc power stage is needed and an active power factor correction (PFC) circuit to meet relevant harmonic standards (e.g., IEC61000-3-2 [17], [18]) is necessary. The purpose of an active PFC circuit is to minimize the input current distortion and to make the current in phase with the input voltage imposing the circuit to behave as a resistive load. Therefore after rectifying the ac line voltage, a dc–dc stage is required.

Conventionally, several stages are used to drive LEDs; a first stage to work as a PFC circuit, and the last one (second or third stage) to control the LEDs current. In [6] several LED driver topologies are introduced and different ac–dc converter candidates to operate as PFC circuits are also presented. In [19], Shrivastava *et al*. propose a single-level dimming concept implemented with current injection technique using a Zeta converter. In [20], a zero current switching isolated LED driver based on a SEPIC-flyback converter without electrolytic capacitor was

Manuscript received July 29, 2016; revised October 30, 2016 and November 24, 2016; accepted December 10, 2016. This work was supported in part by the Spanish Ministerio de Ciencia e Innovación under Grant DPI2013-47293-R. The work of A. El Aroudi and M. AL-Numay was supported by the Visiting Professor Program of King Saud University, Riyadh, Saudi Arabia.

M. Bodetto, A. El Aroudi, and A. Cid-Pastor are with the Group of Automatic Control and Industrial Electronics, Department d'Enginyeria Electrónica, Eléctrica i Automática, Universitat Rovira i Virgili, 43007 Tarragona, Spain (e-mail: mirko.bodetto@urv.cat; abdelali.elaroudi@urv.cat; angel.cid@urv.cat).

M. Al-Numay is with the Department of Electrical Engineering, King Saud University, Riyadh 12372, Saudi Arabia (e-mail: alnumay@ksu.edu.sa).

Color versions of one or more of the figures in this paper are available online at http://ieeexplore.ieee.org.

Digital Object Identifier 10.1109/TIE.2017.2652370

considered. In [21], Huang-Jen *et al.* present a dimmable LED driver with adaptive feedback control for low-power lighting applications.

Single-stage ac–dc converter topologies for PFC are preferred in LED driving because of their simple power circuitry and simple control. It has to be pointed out that using a hysteresis control, the input current $i_{\rm in}(t)$ must be a continuous (non pulsating) function of time, this implies that the current in the input port of the dc–dc converter must be an inductor current. The boost converter, which is the simplest topology fulfilling this requirement and which is the commonly chosen system to perform PFC for many applications, cannot be applied in this case because it only allows step-up operation. Typically, the LEDs voltage $V_{\rm LED}$ is smaller than the maximum value of the time varying line voltage, the converter topology should have the ability to step-up and step-down the input voltage in order to raise or lower the rectified voltage to obtain the appropriate dc voltage value. To improve the power quality in single-stage ac–dc LED drivers, high-order PFC topologies such as Sheppard–Taylor [22], SEPIC and modified SEPIC [23], and Ćuk and modified Ćuk (with an additional diode in series with the output inductor) [24] can be used. The last topology having the advantages of the Ćuk converters, such as a nonpulsating input current, a nonpulsating output current, minimum storage elements, minimum switch number, and high energy storage density using a capacitor instead of an inductor [25], and allowing at the same time a better input current tracking near the zero crossing area of the input voltage [24] is considered the optimum topology and will be used in this work to illustrate the performances of the novel modulation strategy proposed in this paper. It should be noted that, in LED driving applications, because it is the output current that is used to drive the LED, an inductor current must also exist in the output port of the converter being the inverted polarity of the output voltage in all Ćuk converters not a drawback since it will only imply connecting the LED lamp in the backward direction.

In most of the studies, fixed frequency modulation techniques are used. However, variable frequency control techniques such as critical mode control, hysteresis control, and constant ON-time control have also been applied in LED driving applications. For instance, in [26], a single-stage boost converter with high conversion ratio was studied using SiC devices working at the boundary between continuous and discontinuous conduction modes. In [27], a variable ON-time control strategy for a critical conduction mode flyback converter is proposed. In this paper, a variable frequency strategy based on hysteresis modulation is used to design an efficient HBLED driver with PFC in low-power applications. The hysteresis window is modulated by the time varying line input voltage to avoid harmonic distortion close to the zero crossing of the input voltage and also modulated by the output current reference in order to improve the dimming performance of the HBLEDs.

The rest of the paper is organized as follows. After revisiting the problem of power quality at low power levels in ac–dc LED drivers with PFC in Section II, the new technique is described in Section III and its operation principle is presented. The performance of the system under the new control technique is illustrated in Section III by using numerical simulations performed on a system level switched model of the system implemented in PSIM software. These simulations demonstrate the functionality of the proposed technique. A laboratory prototype is also designed and experimental validation of the proposed technique and its practical feasibility is addressed in Section IV, where time domain waveforms and frequency domain spectra demonstrate that the technique is able to provide a low THD at very low power levels. Finally, the conclusions of this study are collected in Section V.

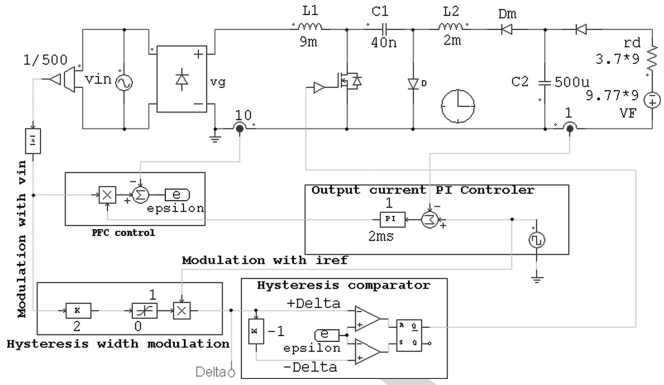

Fig. 1. PSIM schematic diagram of the proposed system.

II. Problem Statement

The luminous flux of HBLEDs is determined by their forward current and therefore, a constant current regulation is needed to achieve constant brightness of HBLEDs. Dimming is another highly desirable requirement for these devices. However, dimmable HBLED drivers exhibit a remarkable increase in the input current THD [28], [30]. Although each individual HBLED driver meets the IEC 61000-3-2 class C standards [8] in commercial or industrial applications, many lamps are combined in series/parallel and used resulting in a high THD. Variable frequency control techniques such as hysteretic control and constant ON-time control have the advantages of fast system response in front of parameter changes. The drawback of using hysteretic control with a fixed hysteresis window is that the switching frequency is variable and reaches very low values near the zero crossing area of the input voltage. This decrease in the switching frequency in this area provokes a harmful harmonic distortion. To mitigate this problem, a technique has been introduced in [28], which consists of modulating the hysteresis window near the zero crossing area of the input voltage. While the technique works quite well for relatively high values of the input current/power, when the system is dimmed at low current/power, an increase in its THD is observed. The system that will be used to illustrate the problem of harmonic distortion and the proposed solution is the modified Ćuk converter reported in [24]. The numerical simulations presented in this section are obtained from PSIM software. The PSIM schematic circuit diagram of the system with the inner and the outer current controllers is shown in Fig. 1. First, the modulation of the hysteresis window will be disabled. The same scheme can be used for simulating the system with conventional hysteresis control

TABLE I
DESIGN SPECIFICATIONS AND PARAMETER VALUES FOR THE ĆUK LED DRIVER

Component	Value
Input voltage	$v_{\rm in} = 230$ V rms
$9 \times$ HBLED, Cree, Inc. "Xlamp MC-E" (Cool White)	$V_F \approx 100$ V, $r_d \approx 30\,\Omega$, $P_o =$ 45 W, $I_{\rm nom} = 350$ mA
L_1	10 mH
L_2	2 mH
C_1	40 nF
C_2	500 μF
$_g = ks\ G\ k_s$: gain of the voltage sensor	P_o=45 W, $g = Po/V_{g,\rm rms}^2 =$ 1/1000 k_s = 1/5000, $G_{\rm REF} \approx 5$ S
Δ: Modulated hysteresis width	10% I_1 @$I_{\rm nom} \rightarrow \Delta i_1 = 30$ mA

by making the hysteresis width constant. The system is supplied by an input voltage $v_{\rm in} = 220$ V rms @ 50 Hz. The load consists of a string of nine serial HBLEDs of "Xlamp MC-E" (Cool White) of Cree, Inc., whose nominal load currents are 350 mA, as detailed in Table I. The nominal value of the output power of 45 W with a corresponding output LED current at 300 mA. When a user wants a dimmed power, the admitted range is between 5% and 120% of the output current. The allowed ripples for the inductor currents and capacitor voltages are between 5% and 10%. The intermediate capacitor is responsible for transferring energy between the input and the output ports, and therefore it must have a low capacitance value. Finally, the output capacitor is responsible for filtering the ripple corresponding to twice the line frequency, hence it will be an electrolytic capacitor with a relatively high value of capacitance. Using the expressions detailed in [29], the design specifications leads to the parameters depicted in Table I. The system is under a hysteretic inner current loop shaping the input current according to a template provided by the product of the input voltage $v_{\rm in}$ and a conductance g given by the outer current loop regulating the LED current. The outer loop consists of a PI controller whose time constant $\tau_i = 2.86$ ms and proportional gain $\kappa_p = 1$ have been selected to get a 66° of phase margin at a crossover frequency of 36 rad/s. The controller parameters were designed by using a simple averaged model. Since the design is for a low-power application, with a relatively high input voltage, the system may operate with very low rms current values.

Each LED can be modeled by its dynamics resistance $r_d = 3.28\ \Omega$ in series with its forward voltage $V_F = 9.77$ V. Fig. 2 shows the waveform of the input current of the system controlled by two different hysteresis control techniques. The first one uses a conventional constant hysteresis width. The second one uses a hysteresis window modulated by only the input voltage $v_{\rm in}$. The results in Fig. 2 show the input variables $i_{\rm in}$ and $gv_{\rm in}$, output current $i_{\rm ref} = I_{\rm LED}$, and the hysteresis window Δ for two different values of output currents $I_{\rm LED} = 100$ mA and $I_{\rm LED}$=20 mA. As can be observed, for constant hysteresis width, harmonic distortions are exhibited near the zero crossing area of the input voltage [see Fig. 2(a)]. These distortions are more pronounced for low output current/power levels [see Fig. 2(b)]. With a hysteresis window modulated by the input voltage, the problem of harmonic distortion is alleviated for relatively high current levels [see Fig. 2(c)] but not for low values of the output LED current [see Fig. 2(d)].

III. NEW TECHNIQUE FOR IMPROVING DIMMING PERFORMANCE OF HBLEDS DRIVERS

To mitigate the increase in the THD problem even at low power levels, a new technique is proposed, which consists of adding an extra feedforward loop in the control stage to adapt the hysteresis window Δ, using the HBLEDs forward current reference.

A. Description of the Control Technique

The new control strategy works according to the block diagram depicted in Fig. 3. The control strategy is given by a hysteretic control law with the following expression:

$$u(t) = \begin{cases} 0, & \text{if } \varepsilon(t) > +\Delta \text{ or } |\varepsilon(t)| < \Delta \text{ and } \varepsilon(t^-) = +\Delta \\ 1, & \text{if } \varepsilon(t) < -\Delta \text{ or } |\varepsilon(t)| < \Delta \text{ and } \varepsilon(t^-) = -\Delta \end{cases} \quad (1)$$

where $\varepsilon = gv_{\rm in} - i_1$ is the input current error, which is also the input to the hysteresis controller, and t^- is the last instant when the control signal hit the switching boundaries defined by $\pm\Delta$. To avoid the harmonic distortion close to the zero crossing of the input current for all current levels $i_{\rm ref}$, the hysteresis window was modulated by the time varying line input voltage $v_{\rm in}$ and a second modulation was applied in terms of the load current reference $i_{\rm ref}$. Therefore, the hysteresis width Δ can be expressed according to the following expression:

$$\Delta(t) = \begin{cases} \alpha v_{\rm in}(t) i_{\rm ref}, & \text{if } \alpha v_{\rm in}(t) i_{\rm ref} < \Delta_{\max} i_{\rm ref} \\ \Delta i_1\, i_{\rm ref}, & \text{if } \alpha v_{\rm in}(t) i_{\rm ref} > \Delta_{\max} i_{\rm ref} \end{cases} \quad (2)$$

where α is a suitable constant gain and $\Delta_{\max}$ is the maximum allowed hysteresis width when modulation with the current reference is not present. The waveforms of the modulated hysteresis window $\Delta(t)$ is depicted in Fig. 4. Because during one switching cycle, the waveforms of the error signal ε can be considered triangular, the switching frequency f_s can be derived as follows:

$$f_s = \frac{1}{T} = \frac{1}{t_{\rm on} + t_{\rm off}} = \frac{1}{2h} \frac{m_{\rm on} m_{\rm off}}{m_{\rm on} + m_{\rm off}} \quad (3)$$

with $m_{\rm on}$ and $m_{\rm off}$ being, respectively, the slopes of the control signal ε for $u = 1$ and for $u = 0$. By substituting the expressions of these slopes in (3), the following expression for the switching frequency is obtained:

$$f_s(t) = \frac{v_{\rm in}(t) v_2}{2\Delta(t)(v_{\rm in}(t) + v_2)} \quad (4)$$

where v_2 is the output voltage. Therefore, the values of α and $\Delta_{\max}$ can be selected in such a way that the switching frequency be within a specified desired range. According to (4), a minimum switching frequency is obtained close to $t = \pi/\omega_l$ (ω_l is the angular line frequency) and a maximum frequency is obtained close to the zero crossing area. Note that, like in a conventional hysteretic controller, the switching frequency depends on the hysteresis width $\Delta(t)$. However, in the conventional strategy,

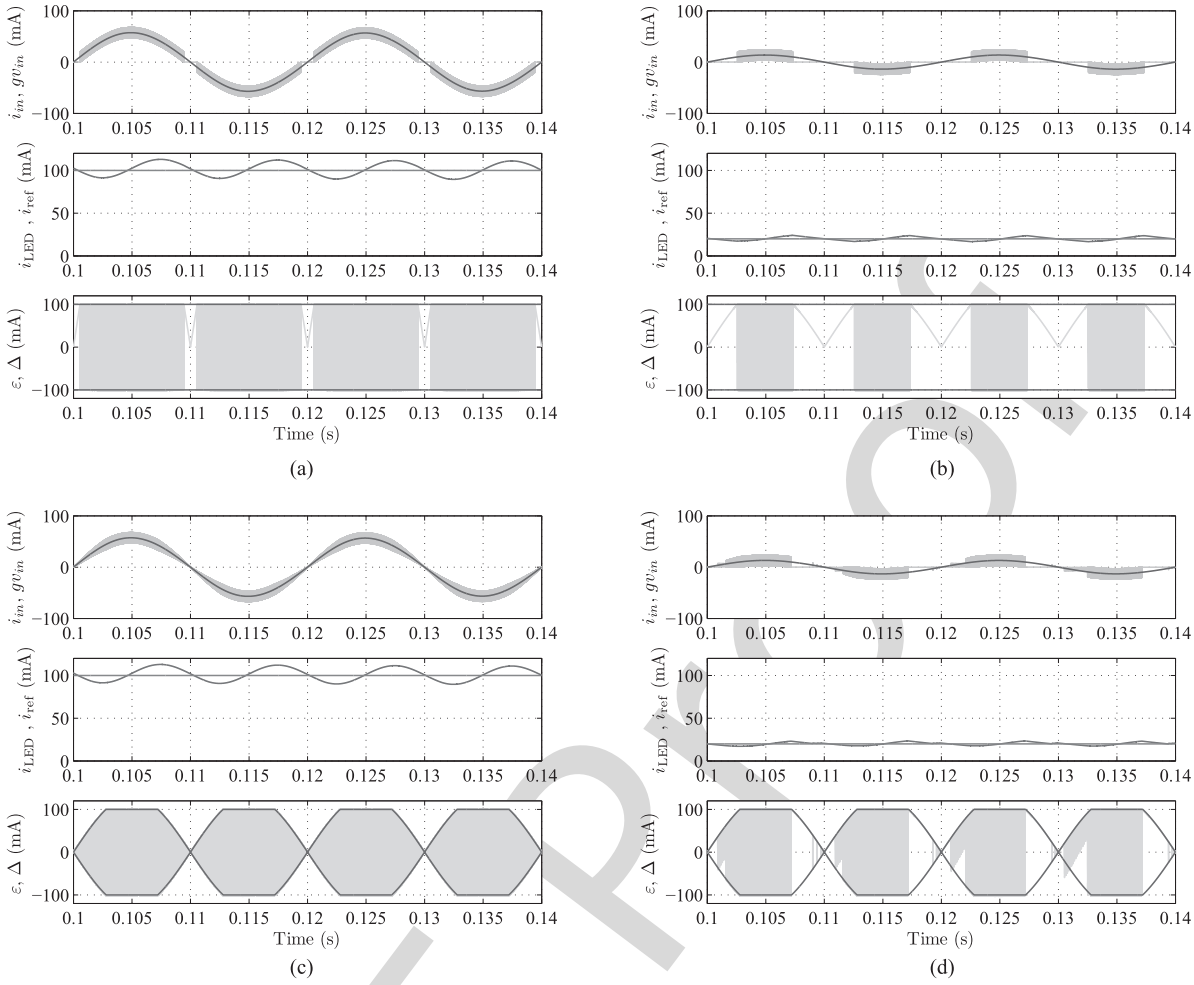

Fig. 2. Waveforms of the Ćuk HBLED driver controlled by hysteresis modulation (only the input voltage is used for the modulation), input variables $i_{\rm in}$ and $gv_{\rm in}$, output current: $I_{\rm LED} = i_{\rm ref}$, hysteresis width for (left): $I_{\rm LED}$ = 100 mA, (right): $I_{\rm LED}$ = 20 mA.

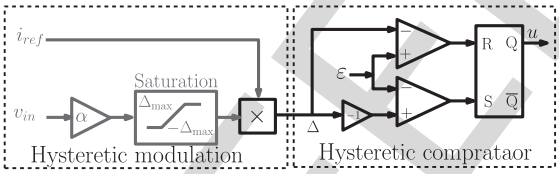

Fig. 3. Block diagram of the new technique.

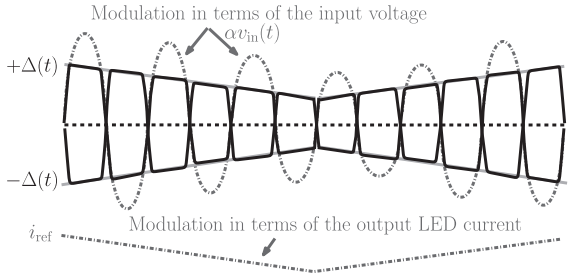

Fig. 4. Evolution of the modulated hysteresis window $\Delta(t)$ in terms of the input voltage and the output LED current. Near the zero crossing area, the hysteresis width shrinks periodically to zero whatever is the value of $i_{\rm ref}$. Far away from the zero crossing area of the input voltage, the hysteresis width is proportional to the current reference $i_{\rm ref} = I_{\rm LED}$ and the input voltage $v_{\rm in}$.

the switching frequency reaches very low value near the zero crossing area causing harmonic distortion. With the proposed double modulation scheme, these distortions are alleviated and the power quality is significantly improved.

B. Validation of the Technique Using Numerical Simulations

With the aim of verifying the previous proposed technique, time-domain numerical simulations performed on a system-level switched model implemented in PSIM software are first presented here.

To avoid the distorting effects when $i_{\rm ref}$ decreases, the new technique shown in Fig. 3 is used. The results are depicted in Fig. 5 where contrarily to the results shown in Fig. 2, a good proportionality between the input variables can be appreciated even for low power levels. In particular, it can be observed that modulating the hysteresis window according to the load reference improves the waveforms quality providing a clean input current and yielding an improvement in the power factor and a decrease in the THD even when the HBLED current

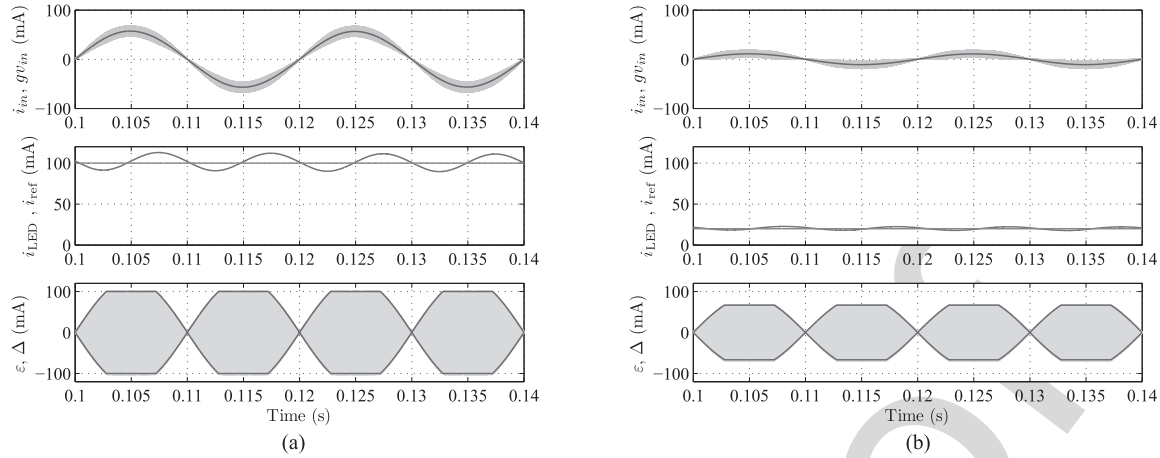

Fig. 5. Waveforms of the Ćuk HBLED driver controlled by the new technique, input variables $i_{\rm in}$ and $gv_{\rm in}$, output current: $I_{\rm LED} = i_{\rm ref}$, hysteresis window for (left): $I_{\rm LED} = 100$ mA, (right): $I_{\rm LED} = 20$ mA.

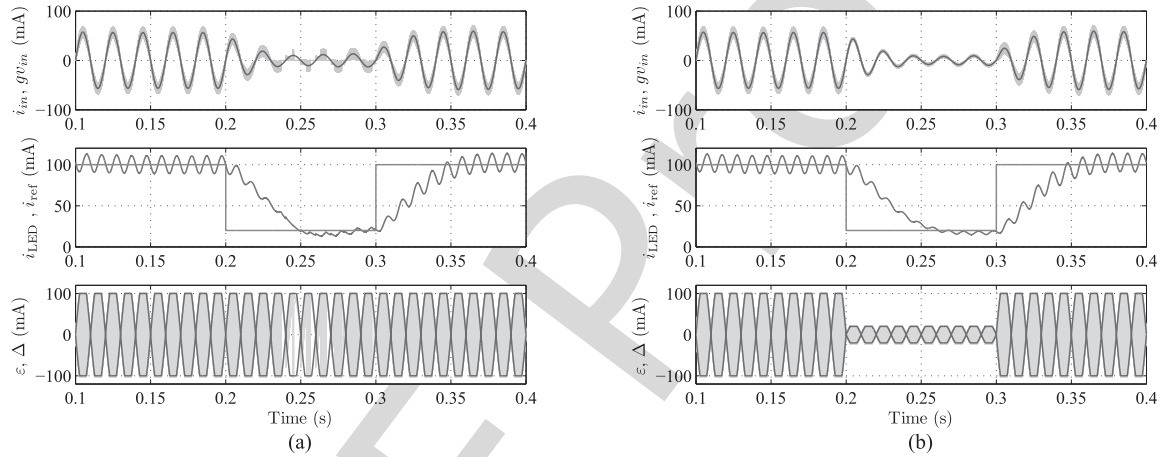

Fig. 6. System responses under (a) hysteresis control with a hysteresis window modulated by the input voltage; and (b) hysteresis control with a hysteresis window modulated by the input voltage and the current reference for different levels of this reference.

is lower than 6% of its nominal value. Hence, a significant improvement in the system performance at low current/power [see Fig. 5(b)] can be obtained.

The evolution of the doubly modulated hysteresis window is also depicted at the bottom of Fig. 5. For the sake of comparison, in Fig. 6, the system responses under hysteresis control with a hysteresis window modulated only by the input voltage and that with the new technique are shown for different levels of the LEDs current reference. One can note that while similar system transient responses are obtained for both control strategies, the second control with doubly modulated hysteresis window outperforms the first one for low power values in the steady-state regime. It should be noted that the fact that the same transient response is obtained for both control schemes means that the system stability is unaltered by the introduction of the new modulation scheme and that conventional techniques based on averaging and linearization procedures can be used for designing the closed-loop system under the proposed control strategy. In fact, the same procedures were applied to design the system with a 66° of phase margin at a crossover frequency of 36 rad/s as in Section II.

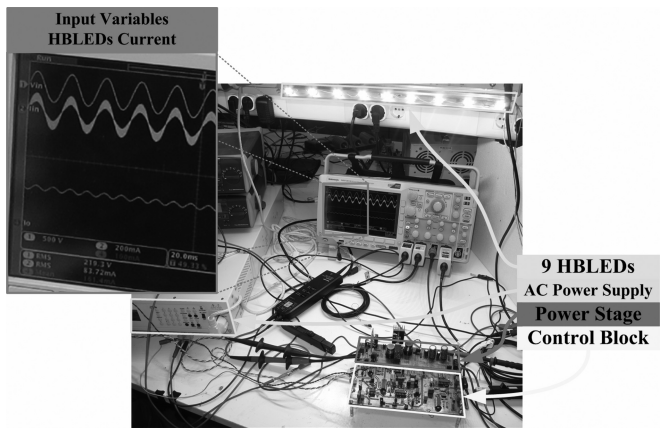

Fig. 7. Photograph of the implemented experimental prototype of a Ćuk LED driver with a hysteresis control.

IV. Experimental Results

The experimental laboratory prototype is depicted in Fig. 7 and its parameters are the same as those listed in numerical

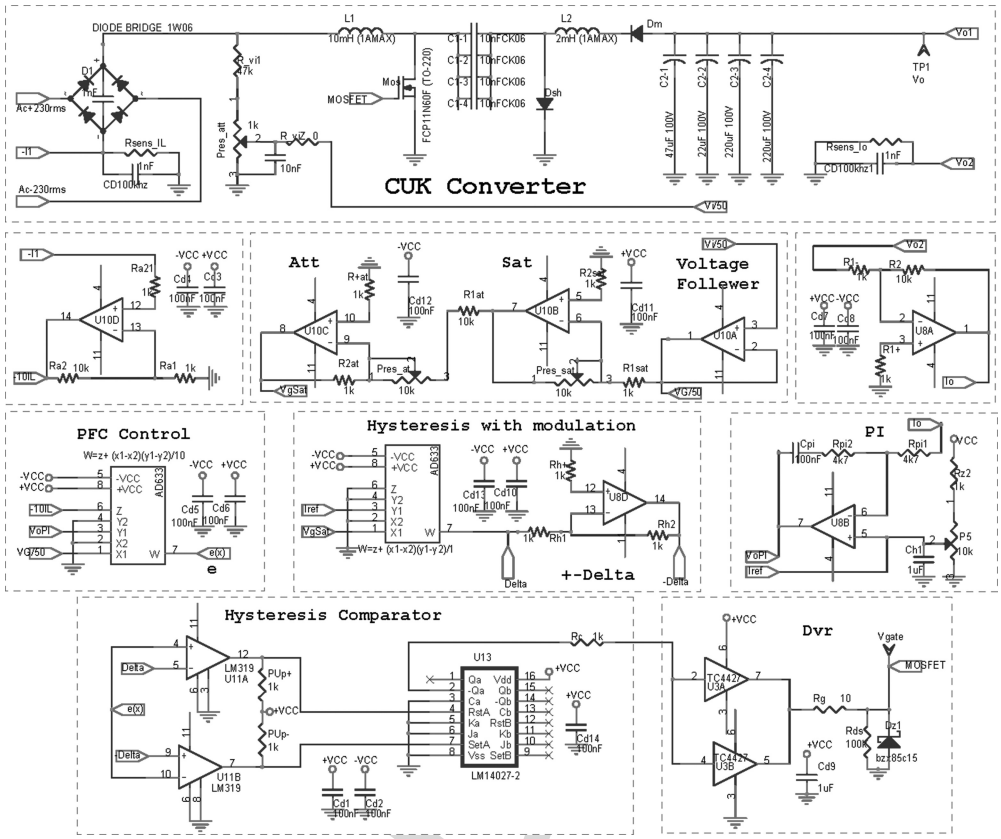

Fig. 8. OrCAD circuit schematics of the implemented modified Ćuk converter and the proposed double modulation strategy.

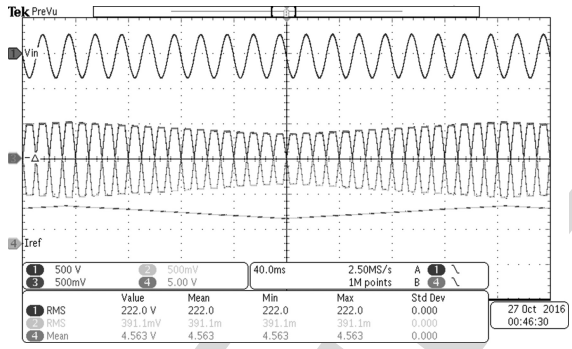

Fig. 9. Waveforms of the hysteresis window when modulated by the sinusoidal input voltage with a saturator block and a triangular output current reference.

simulations (see Table I) and its corresponding OrCAD schematics is shown Fig. 8.

The experimental waveforms corresponding to Fig. 4 are depicted in Fig. 9, where a modulation of the hysteresis window in terms of the input voltage and the output current reference can be observed.

In this section, the results obtained from the modified Ćuk converter LED driver prototype are summarized. The new modulation scheme is implemented according to the block diagram of Fig. 3 using analog devices. The conductance g is given by $g = Gk_s$, where the value of k_s is determined by $k_s = k_v/(\mathrm{AttAD633} \times k_i)$, being k_v the voltage sensor gain ($k_v = 1/50$), k_i the current sensor gain ($k_i = 10$), and AttAD633 the attenuation (AttAD633 $= 10$) of the analog multiplier AD633. Thus, the value of k_s is 1/5000, which was chosen with the aim of obtaining a wider range of control in the power transfer; and consequently a greater control over the load current. As a power source, an ac power supply (Pacific power source model 118acx-upc1) was used instead of the grid. As in the results corresponding to the numerical simulations, the rms value was 220 V and its frequency was $f_l = 50$ Hz. The same load was also used consisting of a string of nine serial HBLEDs of "Xlamp MC-E" (Cool White) of Cree Inc. whose nominal current is 350 mA. A bank of electrolytic capacitors of 500 μF was used at the output of the converter. The inductors were provided by Panasonic Electronics Component ELC18Bxxx. Their inductances have the same nominal values as for the theoretical and simulations results presented previously, i.e., $L_1 = 10$ mH and $L_2 = 2$ mH. The intermediate capacitor $C_1 = 40$ nF, 500 V is a bank of multilayer Ceramic capacitor. The power MOSFET is a Fairchild semiconductor FCP11N60F with a rated voltage of 650 V. The diodes used are Silicon Carbide (SiC) Schottky diodes (IDD04SG60C Infineon) with a VRRM voltage of 650 V. For precise current sensing, resistors with 0.1 Ω were used together with the operational amplifiers MCP6044 for obtaining the required gains. An analog multiplier (AD633JNZ) was used for the control and modulation block that requires a parameterized input voltage and the load current reference to generate the doubly modulated signal Δ. This signal and its opposite are compared to the error signal ε by means of two comparators

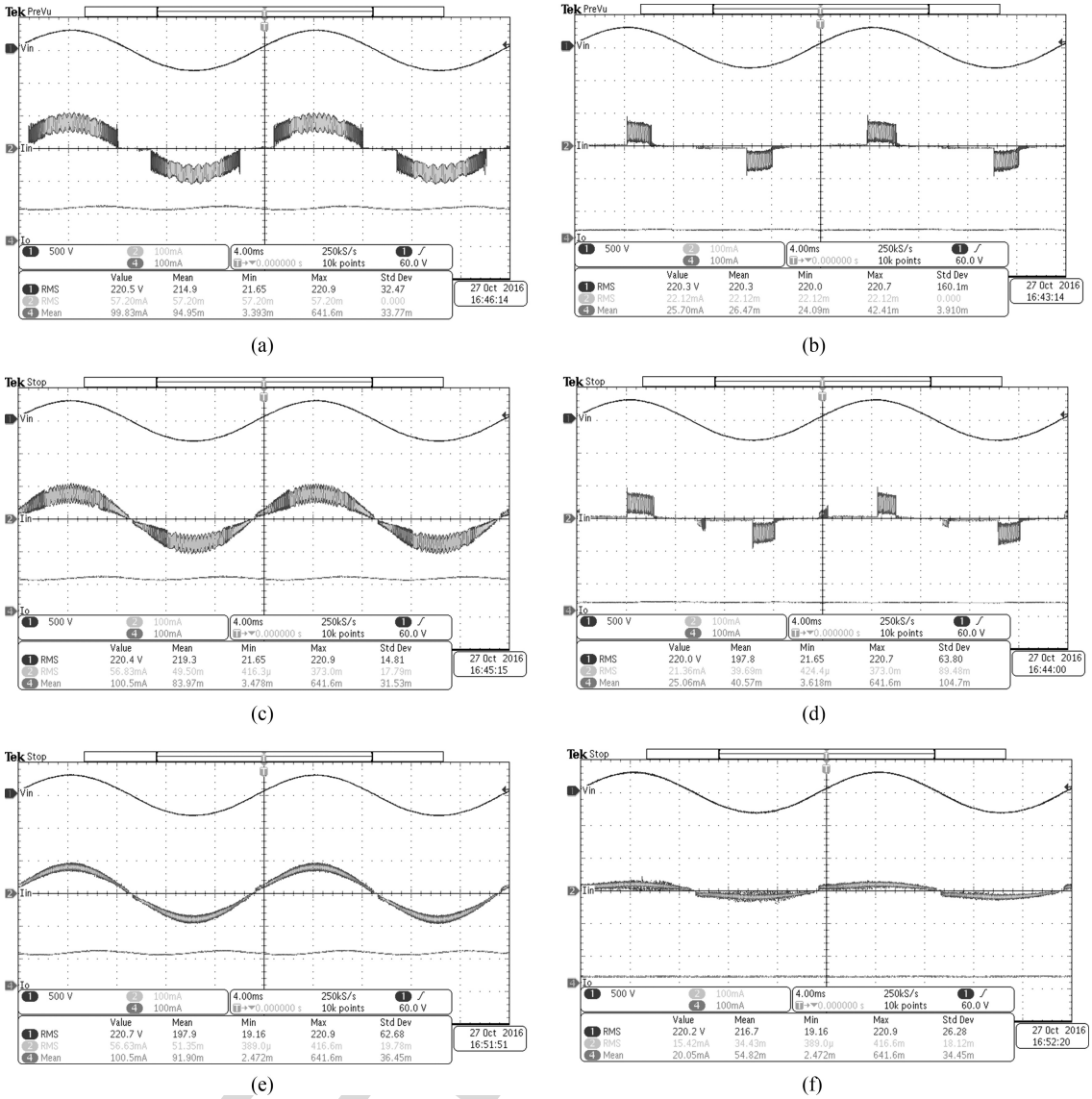

Fig. 10. Experimental measurements of a dimmable Ćuk HBLED driver with LED output current $i_{\rm ref} = 100$ mA (left) and $i_{\rm ref} = 20$ mA (right). (a) and (b) Fixed hysteresis width; (c) and (d) hysteresis control with a hysteresis window modulated by the input voltage; and (e) and (f) hysteresis control with a hysteresis window modulated by the input voltage and the current reference (new technique).

(LM319N) and a SR latch was used to generate the binary signal u that drives the MOSFET (FCP11N60F). The driver used was TC4427.

Fig. 10 show the experimental steady-state system responses for three different modulation schemes and under two different power levels or equivalently output current reference $I_{\rm LED} = i_{\rm ref}$. The panels a, c, and e in this figure correspond to an output current $i_{\rm ref} = 100$ mA while the panels b, d, and f correspond to $i_{\rm ref} = 20$ mA. The top panels correspond to the conventional fixed hysteresis window. The ones on the middle correspond to a hysteresis modulation with a window modulated by only the input voltage. The bottom ones correspond to a hysteresis modulation with a window modulated by both the input voltage and the output current reference. The operation points and the parameter values are the same ones used in the PSIM numerical simulations in the previous section. As can be observed, a perfect proportionality between the input current and the input voltage in the new modulation technique, and low harmonic contents are obtained even at $i_{\rm ref} = 20$ mA, that is less than 6% of the nominal HBLED forward current. The results obtained show a perfect proportionality between the input port variables, without significant harmonic content. Using the new technique, a very low THD is obtained and a wide dimming range is guaranteed. For comparison, Table II shows the THD values, their absolute and relative improvements for the three different control schemes under two current/power conditions. In the worst case ($i_{\rm ref} = 20$ mA) an improvement of 60% and a relative improvement of 80% have been obtained. It is worth to note that when the proposed modulation of the hysteresis window is not applied and with low values of the output current, the LED lamps start causing an annoying flickering. This is because the caused distortions in the input current propagate through the

TABLE II
THD AND ITS RELATIVE IMPROVEMENTS

Load current	I_{LED}	100 mA	20 mA
THD	Fixed hysteresis window	15.8%	82.0%
	Input modulated hysteresis window	5.3%	75.0%
	Input and reference modulated hysteresis window	3.4%	14.5%
Relative improvement		35.85%	80.67%

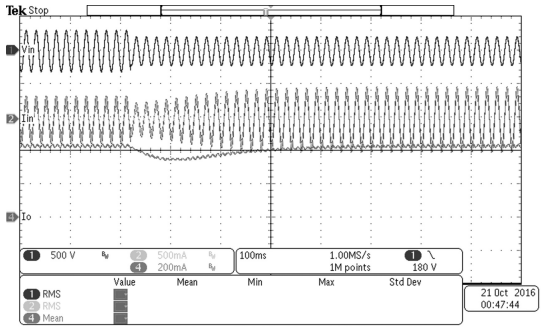

(a)

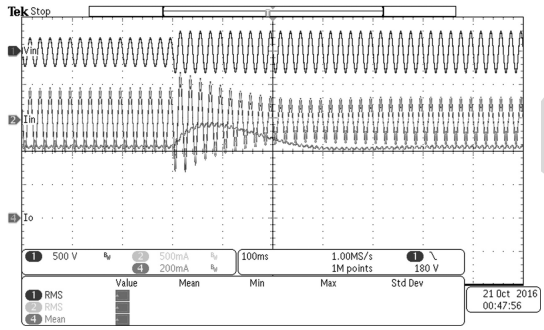

(b)

Fig. 11. Response of the system to step changes in the line voltage from 220 to 150 V rms. (a) From 150 to 220 V rms. (b) From 220 to 150 V rms.

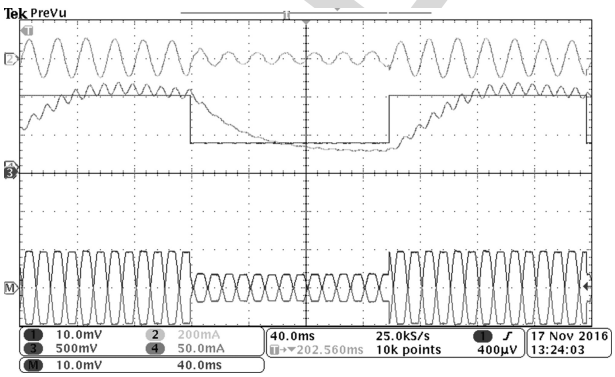

Fig. 12. Response of the system to step changes in the operating load current.

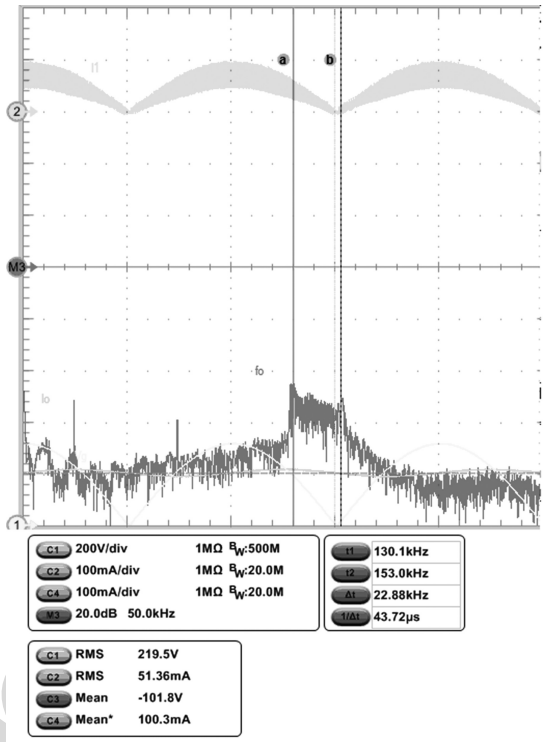

(a)

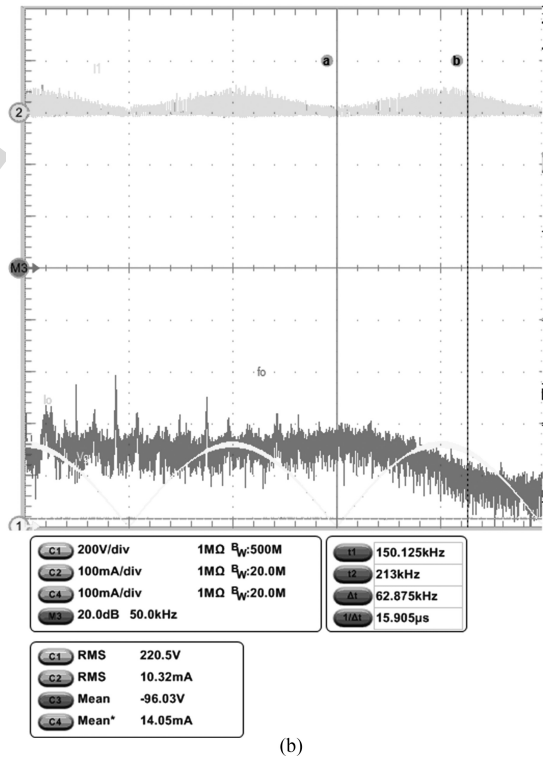

(b)

Fig. 13. FFT spectra corresponding to I_{LED} =100 and 14 mA.

system to output port and a distortion in the HBLED current ripple takes place and starts to reach unacceptable values. With the proposed technique all of these effects are avoided.

To check the robustness of the system against line disturbance, step changes were applied in the input voltage amplitude from 220 to 150 V rms and vice versa. These step changes can represent dips in the grid. The corresponding system responses are shown in Fig. 11. To test the system response to step changes in the operating load current, a periodic square wave signal was also applied to the output current reference

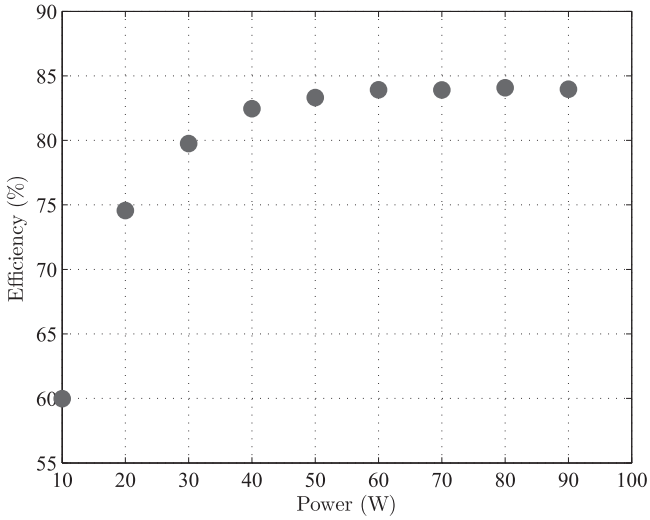

Fig. 14. Efficiency of the Ćuk LED driver for different power levels.

using the function generator GFG 2004 from ISO-TECH. The corresponding response is shown in Fig. 12. All the tests demonstrate the robustness of the technique against changes in the grid and the load. The FFT spectra depicted in Fig. 13 correspond to the input line current for two different values of the power conditions corresponding to $I_{\rm LED}$ =100 and 14 mA, the second case representing a 4% of $I_{\rm nom}$ = 350 mA. Additionally, the standards IEC61000-3-2, class C norms [17], [18] are checked to be met. Finally, Fig. 14 shows the efficiency of the system for different power levels. It can be observed that the implemented prototype reaches an efficiency of 75% at a power level of 20 W and 84% for a power level between 50 and 100 W. Compared with [20, Fig. 12], at low power levels and with similar rms value of the input voltage, the proposed technique shows comparable efficiency. In [20], a better efficiency was obtained at relatively high power levels between 50 and 100 W. However, the efficiency at this range of power depends on the switching devices used and the optimization of other aspects, such as the reactive components and many other factors, but not on the modulation strategy used, which is the main focus of the present study.

V. Conclusion

The harmonic distortion under low-power dimming conditions can cause harmful effects in single-stage high-order LED drivers with PFC under variable frequency hysteresis control, and hence can provoke serious power quality problems on the ac line and also annoying flickering of the lamps. In this paper, a new modulation technique based on a time-varying hysteresis width was proposed to solve this problem. Modulating the hysteresis window by an extra feedforward loop in the control stage, using the current reference, has been shown to decrease the THD of HBLED drivers under low current/power conditions, and hence improving the dimming performance of the ac–dc LED driver. By using the new technique, a very low THD is obtained and a wide dimming range is guaranteed. The topology of the modified Ćuk converter was built to verify the proposed control strategy. The experiments performed in the laboratory for the proposed control verify the theoretical and simulation results, which corroborate the correct operation of the proposed control strategy. Moreover, the performance of the new technique algorithm was compared with conventional and already existing strategies. The comparison shows that the new control method is a robust technique and is compatible with the standards IEC61000-3-2, class C norms at low power levels. Hence, the results presented in this paper provide a new way for improving the dimming performance of low power single-stage ac–dc HBLED drivers. The technique can be applied to any ac–dc PFC topology where a hysteresis switching decision is used and the switching function have a triangular shape.

Acknowledgment

The authors would like to thank the anonymous reviewers for providing comments and suggestions that helped in improving a first version of this paper.

References

[1] M. Hansen, Energy-efficient lighting lifecycle. 2009. [Online]. Available: Available at: http://www.cree.com/
[2] D. Gacio, J. M. Alonso, A. J. Calleja, J. Garcia, and M. Rico-Secades, "A universal-input single-stage high-power-factor power supply for HB-LEDs based on integrated buck-flyback converter," *IEEE Trans. Ind. Electron.*, vol. 58, no. 2, pp. 589–599, Mar. 2011.
[3] M. R. Krames, "Status and future of high-power light-emitting diodes for solid-state lighting," *J. Display Technol.*, vol. 3, pp. 160–175, Jun. 2007.
[4] L. C. Kwan, L. Sinan, and S. Y. Hui, "A design methodology for smart LED lighting systems powered by weakly regulated renewable power grids," *IEEE Trans. Smart Grid*, vol. 2, no. 3, pp. 548–554, Aug. 2011.
[5] Y. Zhongming, F. Greenfeld, and L. Zhixiang, "Design considerations of a high power factor SEPIC converter for high brightness white LED lighting applications," in *Proc. IEEE Power Electron. Spec. Conf.*, 2008, pp. 2657–2663.
[6] M. Arias, A. Vázquez, and J. Sebastián, "An overview of the AC-DC and DC-DC converters for LED lighting applications," *Automatika J. Control, Meas., Electron., Comput. Commun.*, vol. 53, pp. 156–172, Feb. 2012.
[7] Y. K. Lo, K. H. Wu, K. J. Pai, and H. J. Chiu, "Design and implementation of RGB LED drivers for LCD backlight modules," *IEEE Trans. Ind. Electron.*, vol. 56, no. 12, pp. 4862–4871, Dec. 2009.
[8] J. M. Alonso, J. Viña, D. G. Vaquero, G. Martínez, and R. Osorio, "Analysis and design of the integrated double buck-boost converter as a high-power-factor driver for power-LED lamps," *IEEE Trans. Ind. Electron.*, vol. 59, no. 4, pp. 1689–1697, Apr. 2012.
[9] L. Dong *et al.*, "Enhancement of thermal conductivity of die attach adhesives (DAAs) using nanomaterials for high brightness light-emitting diode (HBLED)," in *Proc. 61st IEEE Electron. Components Technol. Conf.*, 2011, pp. 667–672.
[10] G. Shan, H. Jupyo, S. Sanghyun, L. Yongki, C. Seogmoon, and Y. Sung, "Design optimization on the heat transfer and mechanical reliability of high brightness light emitting diodes (HBLED) package," in *Proc. 58th IEEE Electron. Components Technol. Conf.*, 2008, pp. 798–803.
[11] A. Chakraborty, L. Shen, and U. K. Mishra, "Interdigitated multipixel arrays for the fabrication of high-power light-emitting diodes with very low series resistances, reduced current crowding, and improved heat sinking," *IEEE Trans. Electron Devices*, vol. 54, no. 5, pp. 1083–1090, May 2007.
[12] S. Y. Hui and Y. X. Qin, "A general photo-electro-thermal theory for light emitting diode (LED) systems," *IEEE Trans. Power Electron.*, vol. 24, no. 8, pp. 1967–1976, Aug. 2009.
[13] C. Biber, "LED light emission as a function of thermal conditions," in *Proc. IEEE Semicond. Thermal Meas. Manage. Symp.*, 2008, pp. 180–184.
[14] Z. Jianmin and Y. Wei, "Experimental investigation on the performance characteristics of white LEDs used in illumination application," in *Proc. IEEE Power Electron. Spec. Conf.*, 2007, pp. 1436–1440.

[15] G. Sauerlander, D. Hente, H. Radermacher, E. Waffenschmidt, and J. Jacobs, "Driver electronics for LEDs," in *Proc. IEEE Ind. Appl. Soc. Annu. Meeting*, 2006, pp. 2621–2626.
[16] D. Gacio, J. M. Alonso, J. Garcia, M. S. Perdigao, E. S. Saraiva, and F. E. Bisogno, "Effects of the junction temperature on the dynamic resistance of white LEDs," *IEEE Trans. Ind. Appl.*, vol. 49, no. 2, pp. 750–760, Mar./Apr. 2013.
[17] *IEEE Recommended Practices and Requirements for Harmonic Control in Electrical Power Systems*, IEEE Std 519-1992, 1993.
[18] *Limits for Harmonic Current Emissions (Equipment Input Current ≤ 16 A Per Phase)*, IEC 61000-3-2, Part 3-2, 3rd ed., 2005.
[19] A. Shrivastava, B. Singh, and S. Pal, "A novel wall-switched step-dimming concept in LED lighting systems using PFC zeta converter," *IEEE Trans. Ind. Electron.*, vol. 62, no. 10, pp. 6272–6283, Oct. 2015.
[20] B. Poorali and E. Adib, "Analysis of the integrated SEPIC-flyback converter as a single-stage single-switch power-factor-correction LED driver," *IEEE Trans. Ind. Electron.*, vol. 63, no. 6, pp. 3562–3570, Jun. 2016.
[21] C. Huang-Jen, L. Yu-Kang, C. Jun-Ting, C. Shih-Jen, L. Chung-Yi, and M. Shann-Chyi, "A high-efficiency dimmable LED driver for low-power lighting applications," *IEEE Trans. Ind. Electron.*, vol. 57, no. 2, pp. 735–743, Feb. 2010.
[22] C. K. Tse and M. H. L. Chow, "New single-stage PFC regulator using the Sheppard-Taylor topology," *IEEE Trans. Power Electron.*, vol. 13, no. 5, pp. 842–851, Sep. 1998.
[23] M. Ali, M. Orabi, M. E. Ahmed, and A. El Aroudi, "Design consideration of mdified SEPIC converter for LED lamp driver," in *Proc. 2nd Int. Symp. Power Electron. Distrib. Generation*, Hefei, China, 2010, pp. 394–399.
[24] M. Bodetto, A. Marcos-Pastor, A. ElAroudi, A. Cid-Pastor, and E. Vidal-Idiarte, "Modified Ćuk converter for high-performance power factor correction applications," *IET Power Electron.*, vol. 8, no. 10, pp. 2058–2064, Sep. 2015.
[25] S. C. Tan and Y. M. Lai, "Constant-frequency reduced-state sliding mode current controller for Ćuk converters," *IET Power Electron.*, vol. 1, pp. 466–477, Dec. 2008.
[26] A. Leon-Masich, H. Valderrama-Blavi, J. M. Bosque-Moncusi, J. Maixe-Altes, and L. Martinez-Salamero, "Sliding-mode-control-based boost converter for high-voltage-low-power applications," *IEEE Trans. Ind. Electron.*, vol. 62, no. 1, pp. 229–237, Jan. 2015.
[27] T. Yan, J. Xu, F. Zhang, J. Sha, and Z. Dong, "Variable-on-time-controlled critical-conduction-mode flyback PFC converter," *IEEE Trans. Ind. Electron.*, vol. 61, no. 11, pp. 6091–6099, Nov. 2014.
[28] M. Bodetto, A. ElAroudi, A. Cid-Pastor, J. Calvente, and L. Martinez-Salamero, "Design of AC-DC PFC high-order converters with regulated output current for low power applications," *IEEE Trans. Power Electron.*, vol. 31, no. 3, pp. 2012–2025, Mar. 2016.
[29] J. R. de Britto, A. E. Demian, L. C. de Freitas, V. J. Farias, E. A. A. Coelho, and J. B. Vieira, "A proposal of LED lamp driver for universal input using Ćuk converter," in *Proc. IEEE Power Electron. Spec. Conf.*, 2008, pp. 2640–2644.
[30] K. I. Hwu and W. C. Tu, "Controllable and dimmable AC LED driver based on FPGA to achieve high PF and low THD," *IEEE Trans. Ind. Informat.*, vol. 9, no. 3, pp. 1330–1342, Aug. 2013

Mirko Bodetto was born in Rosario, Argentina, in 1973. He received the graduate degree in electronics engineering, the Master's degree in electronics engineering, and the Ph.D. degree from the Universitat Rovira i Virgili, Tarragona, Spain, in 2010, 2011, and 2015, respectively.

His research interests include the field of power electronics applications, including dc–dc switched power supplies and ac–dc power-factor-correction converters for low-power applications such as solid-state lighting and renewable energy systems.

Abdelali El Aroudi (M'00–SM'13) received the graduate degree in physical science from the Faculté des Sciences, Université Abdelmalek Essaadi, Tetouan, Morocco, in 1995, and the Ph.D. degree (Hons.) in applied physical science from the Universitat Politècnica de Catalunya, Barcelona, Spain, in 2000.

He is a full-time tenured Associate Professor in the Department of Electronics, Electrical Engineering and Automatic Control, Universitat Rovira i Virgili (URV), Tarragona, Spain. His research interests include the field of structure and control of power conditioning systems for autonomous systems, power factor correction, stability problems, nonlinear dynamics, and control.

Dr. Aroudi was a Guest Editor of the IEEE JOURNAL ON EMERGING AND SELECTED TOPICS IN CIRCUITS AND SYSTEMS Special Issue on Design of Energy-Efficient Distributed Power Generation Systems (September 2015). He currently serves as an Associate Editor of *IET Power Electronics* and *IET Electronics Letters*.

Angel Cid-Pastor (M'07) received the graduate degrees in ingeniero en electrónica industrial in 1999 and in ingeniero en automática y electrónica industrial in 2002 from the Universitat Rovira i Virgili, Tarragona, Spain. He received the M.S. degree in design of microelectronics and microsystems circuits from the Institut National des Sciences Appliquées, Toulouse, France, in 2003, and Ph.D. degrees from the Universitat Politécnica de Catalunya, Barcelona, Spain, and from the Institut National des Sciences Appliquées, LAAS-CNRS, Toulouse, France, in 2005 and 2006, respectively.

He is currently an Associate Professor in the Departament d'Enginyeria Electrònica, Eléctrica i Automàtica, Escola Técnica Superior d'Enginyeria, Universitat Rovira i Virgili. His research interests include power electronics and renewable energy systems.

Mohammed S. Al-Numay (M'04) was born in Riyadh, Saudi Arabia. He received the B.S. degree (with honors) from King Saud University, Riyadh, Saudi Arabia, in 1986, the M.S. degree from Michigan State University, East Lansing, MI, USA, in 1990, and the Ph.D. degree from Georgia Institute of Technology, Atlanta, GA, USA, in 1997, all in electrical engineering.

Since 1998, he has been with the Electrical Engineering Department, King Saud University, where he is currently an Associate Professor. During the period 2002–2006, he was the Dean of Admissions and Registration at King Saud University. Since 2008, he has been a Senior Consultant for student information systems and electronic admission for many government and private universities and colleges. He was appointed as the Assistant Vice Rector for Information Technology at King Saud University in 2015. His research interests include modeling and control of switched-mode power supplies.

Queries

Q1. Author: Please provide the graduate degree name.

Q2. Author: Please provide the subject in which and institutional details from where "Mirko Bodetto" received his Ph.D. degree.

Q3. Author: Please provide the statement of current position/affiliation.

Q4. Author: Please provide the graduate degree name.

Q5. Author: Please provide the graduate degree name.

Q6. Author: Please provide the translate subjects of degrees into English.

Q7. Author: Please whether biography of "Angel Cid-Pastor" is ok as set.